

# Femtosecond near-field optical spectroscopy of implantation patterned semiconductors

B. A. Nechay,<sup>a)</sup> U. Siegner, F. Morier-Genoud, A. Schertel,<sup>b)</sup> and U. Keller  
*Swiss Federal Institute of Technology Zurich, Institute of Quantum Electronics, ETH Hönggerberg-HPT,  
 CH-8093 Zürich, Switzerland*

(Received 10 August 1998; accepted for publication 29 October 1998)

We have developed a femtosecond-resolved near-field scanning optical microscope, using a diffraction-limited pump and near-field probe configuration, which allows us to measure carrier dynamics with a spatial resolution of  $\sim 150$  nm and a time resolution of  $\sim 250$  fs. This instrument is used for near-field degenerate pump-probe studies of carrier dynamics in GaAs/AlGaAs single quantum well samples locally patterned by focused-ion-beam (FIB) implantation. We find that lateral carrier diffusion across the nanometer-scale FIB pattern plays a significant role in the decay of the excited carriers. © 1999 American Institute of Physics. [S0003-6951(99)02901-0]

Ultrafast optical spectroscopy has yielded a wealth of information about carrier dynamics in semiconductors.<sup>1</sup> However, conventional far-field techniques give only limited physical information about the properties of nanometer-scale lateral structures since their inherent inhomogeneity cannot be spatially resolved due to diffraction-limited resolution. Furthermore, far-field measurements can tell us little about the transport mechanisms on the submicron lateral scale. In order to circumvent these limitations, far-field ultrafast optical spectroscopic techniques can be combined with the nanometer-scale lateral resolution of optical measurements obtained with near-field scanning optical microscopy (NSOM).<sup>2,3</sup> So far, only very few such efforts<sup>4-7</sup> have been reported. This letter discusses the development of an instrument which combines a femtosecond degenerate pump-probe technique with NSOM. Ultrafast measurements of carrier dynamics in nanometer-scale ion-implanted single quantum well samples prove that information about physical processes can be obtained with a spatial resolution of  $\sim 150$  nm and a time resolution of  $\sim 250$  fs. We find that the decay time around the ion-implanted structures is strongly influenced by lateral carrier diffusion on the nanometer scale. This effect cannot be measured with a far-field system.

The ultrafast NSOM, shown in Fig. 1(a), combines a home-built NSOM with a standard degenerate femtosecond pump-probe setup. The NSOM instrument consists of a standard pulled or etched Al-coated fiber which is scanned across the sample, with tip-to-sample distances kept at  $\sim 10$  nm through shear-force feedback using tuning fork detection.<sup>8</sup> A laser source generates  $\sim 100$  fs pulses at 840 nm. The pump pulse excites carriers globally through the NSOM objective lens. The probe pulse is first precompensated for the group velocity dispersion of the  $\sim 60$  cm NSOM fiber and then transmitted through the NSOM tip and the sample to an avalanche photodiode. The pump and probe beams are acousto-optically modulated at 1 and 1.05 MHz, respectively. Such high frequencies are needed to suppress the transient thermal effects of the tip,<sup>9</sup> and to reduce the

effect of laser noise. Differential probe transmission is measured at the 50 kHz difference frequency versus time delay  $\Delta t$  between the pump and probe pulses using a lock-in technique. The carrier dynamics can then be extracted from this data.

In order to limit shot noise and laser noise, backscattered pump light is minimized by a confocal setup, which reduces the sample area over which light is collected, and by using polarization discrimination. No spectral filtering is needed, avoiding the need for complicated two-color laser setups.<sup>4,7</sup> We are able to measure differential probe transmission below  $10^{-4}$ , despite the low ( $10^{-4}$ – $10^{-5}$ ) power throughput of the NSOM tips.

In order to prove the capabilities of the femtosecond NSOM, we measured two implantation patterned samples. Both samples consist of 80 Å GaAs/Al<sub>0.3</sub>Ga<sub>0.7</sub>As single quantum wells, which were mounted on glass disks and selectively etched to remove the GaAs substrates. The 12 nm thickness of the top Al<sub>0.3</sub>Ga<sub>0.7</sub>As barrier keeps the quantum well within the near field of the tip for optimal spatial resolution. Nanometer-width implantation stripes were laterally patterned on these samples by focused-ion-beam (FIB) im-

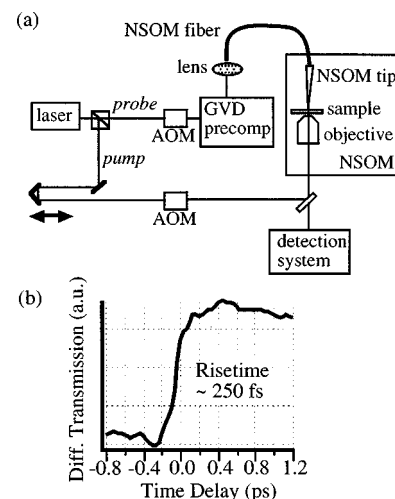


FIG. 1. (a) Experimental setup and (b) near-field pump-probe scan of sample 2, indicating a  $\sim 250$  fs rise time.

<sup>a)</sup>Electronic mail: nechay@iqe.phys.ethz.ch

<sup>b)</sup>Current address: Micrion GmbH, D-85622 Feldkirchen, Germany.

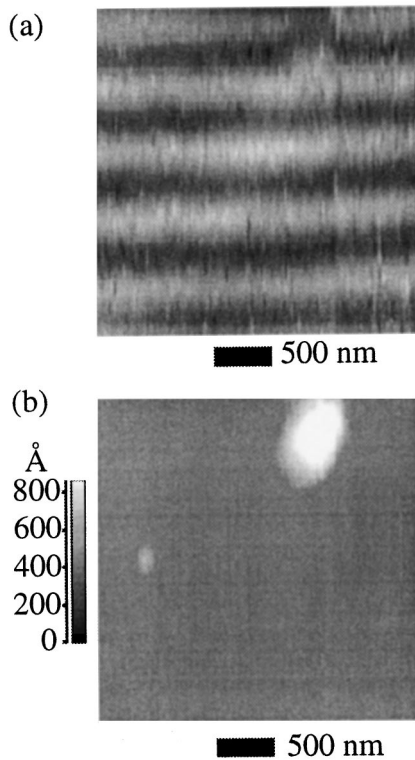


FIG. 2. (a) Variations in the pump-probe amplitude across the area of sample 1. The lighter regions correspond to the larger signal. (b) Simultaneously measured topography.

plantation of Ga ions at 50 keV. In sample 1, the FIB pattern consists of 200 nm implanted stripes at a  $\sim 3 \times 10^{12}$  ions/cm<sup>2</sup> dose with 400 nm spaces between stripes. In sample 2, the pattern consists of 100 nm implanted stripes at a  $\sim 8 \times 10^{11}$  ions/cm<sup>2</sup> dose with 2  $\mu\text{m}$  spaces. All measurements are performed at 300 K, exciting at the band edge with a pump fluence of 4  $\mu\text{J}/\text{cm}^2$ .

Figure 1(b) shows a near-field pump-probe scan of an unpatterned region of sample 2. The 10%–90% rise time demonstrates a time resolution of  $\sim 250$  fs. Figure 2(a) shows a two-dimensional image of the amplitude of the ultrafast pump-probe signal from sample 1 at zero time delay. One can clearly distinguish variations which follow the FIB pattern, where the low signal areas correspond to the high dose implanted stripes, as expected.<sup>10</sup> The topography of the same area, shown in Fig. 2(b), clearly proves that the variation in Fig. 2(a) is purely optical and is not due to topographical artifacts.<sup>11</sup> Significantly, these variations were not observed in the linear probe transmission, demonstrating that these are indeed variations in the optical nonlinearity.

A series of pump-probe time-domain measurements were taken at various positions across the FIB pattern of Fig. 2(a). Figure 3 shows normalized plots of a few of these scans, while the inset of Fig. 3 shows the amplitude of the scans at  $\Delta t = 0$  as a function of distance across the FIB pattern. Taking the 10%–90% variation in the amplitude as the measure of spatial resolution, our data demonstrate a resolution of 150 nm. Furthermore, Fig. 3 shows that the decay time just outside of the implanted stripe is  $\sim 10$  ps, much shorter than the  $\sim 100$  ps decay time of an unpatterned region of the sample. Significantly, the decay time is almost

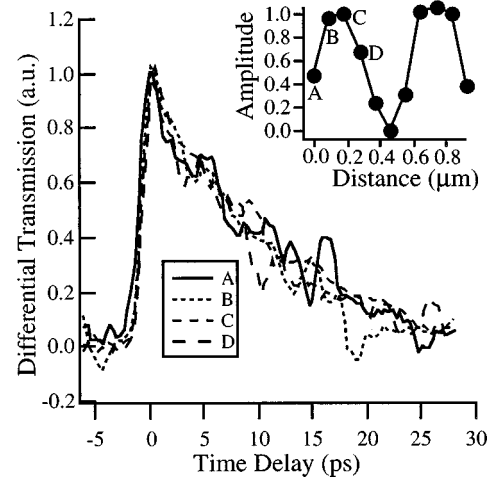


FIG. 3. Normalized pump-probe scans at various points in the pattern of Fig. 2. Inset shows the amplitude of the scans as a function of distance across the pattern.

independent of the position across the FIB pattern, in contrast to the amplitude.

To further explore the spatial dependence of the decay time, near-field pump-probe measurements were performed on sample 2, which had a wider 2  $\mu\text{m}$  spacing that allows us to study carrier dynamics farther away from the FIB stripe. A higher-throughput,  $\sim 300$  nm lateral resolution, NSOM tip was used to obtain better signal to noise within the implanted stripes. Figure 4(a) shows the decay time and amplitude of the pump-probe scans measured versus distance across the FIB pattern. One can see that the decay time is roughly constant over a  $\sim 800$  nm region, while the pump-probe amplitude changes over this region, confirming the results from sample 1.

First we note that the relative flatness of the spatial profile of the decay time cannot be purely due to spatial averaging of the NSOM tip since this would also lead to a flat profile of the amplitude, in disagreement with the experimental result. Moreover, we recall that the carrier trapping time and the amplitude of the differential transmission both in-

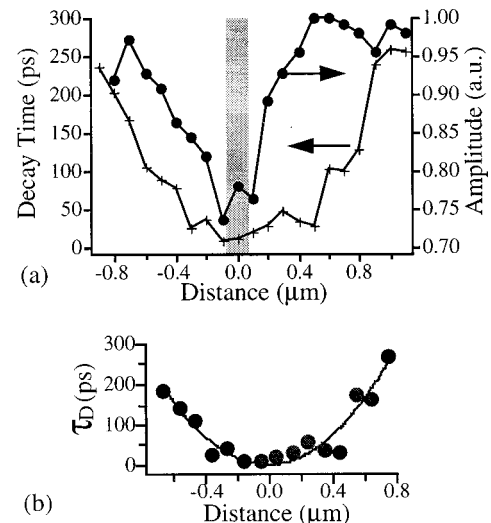


FIG. 4. (a) Decay time (+) and amplitude (●) of measured pump-probe scans across sample 2. The shaded region represents an implanted stripe. (b) Measured diffusion time vs distance (dots) and parabolic fit (solid line).

crease with decreasing implantation dose.<sup>10,12</sup> Therefore, the increase of the amplitude with increasing distance from the implantation stripe shows that the dose decreases, as expected from the implantation parameters. Consequently, the short, almost constant, decay time is not correlated with the implantation dose in this region and cannot be due to trapping of carriers into implantation-induced defects. We conclude that carrier diffusion strongly affects the decay, besides the slow recombination of electron–hole pairs. Diffusion has been shown to affect the decay of carriers in other types of semiconductor nanostructures.<sup>5,6,13</sup> In a simple model, one can assume instantaneous depletion of bands in the implanted stripes due to fast trapping. The resulting gradient in excited carrier density leads to diffusion of excited carriers from the unimplanted regions into the implanted stripes. The measured decay rate of carriers in unimplanted regions is then a sum of diffusion and recombination:  $1/\tau_{\text{meas}} = 1/\tau_D + 1/\tau_R$ , where  $\tau_R$  is the recombination time, measured in an unpatterned region of the sample, and  $\tau_D$  is the diffusion time for a distance  $d$  away from the implanted stripe. The quadratic fit of  $\tau_D = (\tau_{\text{meas}}^{-1} - \tau_R^{-1})^{-1}$  to  $d$ , shown in Fig. 4(b) for sample 2 with  $\tau_R = 250$  ps, strongly supports the role of diffusion.

A simple diffusion model was used to estimate the ambipolar diffusion constant from the measurements of sample 1. This model assumes an initially sinusoidal carrier distribution and a decay rate dominated by diffusion. These assumptions are reasonable for sample 1 since the widths of implanted stripes and spaces are relatively equal and since the measured decay times are much smaller than the 100 ps recombination time. Sample 2 did not meet these requirements since the implanted stripe width is much smaller than the stripe spacing. This model yields an ambipolar diffusion constant of  $8 \text{ cm}^2/\text{s}$ , a reasonable value for III/V materials.<sup>13,14</sup> It is worthwhile to note that, given this diffusion constant, the diffusion within the short  $\sim 200$  fs pulse width is negligible, so that the lateral spread of the pump–probe amplitude is mainly due to tip resolution. This makes the pump–probe amplitude signal useful for qualitative char-

acterization of arbitrary lateral implantation profiles.

In summary, we have developed an ultrafast NSOM with  $\sim 150$  nm lateral and  $\sim 250$  fs temporal resolution and a differential transmission sensitivity below  $10^{-4}$ . No spectral filtering is used, avoiding the need for complicated two-color laser setups. The capabilities of this instrument have been proven through studies of carrier dynamics in focused-ion-beam-implanted samples. We find that lateral diffusion effects can considerably affect carrier dynamics in nanometer-scale patterned structures due to the short length scales involved.

The authors would like to acknowledge Dieter Pohl and Renato Zenobi for access to their NSOM tip fabrication facilities and Hartmut Bielefeldt and Marc Achermann for experimental help. This work was supported by the Swiss National Science Foundation, Program No. NFP 36.

<sup>1</sup>J. Shah, *Ultrafast Spectroscopy of Semiconductors and Semiconductor Nanostructures* (Springer, Berlin, 1996).

<sup>2</sup>D. W. Pohl, W. Denk, and M. Lanz, *Appl. Phys. Lett.* **44**, 651 (1984).

<sup>3</sup>E. Betzig and J. K. Trautman, *Science* **257**, 189 (1992).

<sup>4</sup>J. B. Stark, U. Mohideen, and R. E. Slusher, *Tech. Dig. Ser. Conf. Ed.* **16**, 82 (1995).

<sup>5</sup>S. Smith, N. C. R. Holme, B. Orr, R. Kopelman, and T. Norris, *Ultramicroscopy* **71**, 213 (1998).

<sup>6</sup>J. Levy, V. Nikitin, J. M. Kikkawa, A. Cohen, N. Samarth, R. Garcia, and D. D. Awschalom, *Phys. Rev. Lett.* **76**, 1948 (1996).

<sup>7</sup>A. Vertikov, M. Kuball, A. V. Nurmikko, and H. J. Maris, *Appl. Phys. Lett.* **69**, 2465 (1996).

<sup>8</sup>K. Karrai and R. D. Grober, *Appl. Phys. Lett.* **66**, 1842 (1995).

<sup>9</sup>A. H. Rosa, B. I. Yakobson, and H. D. Hallen, *Appl. Phys. Lett.* **67**, 2597 (1995).

<sup>10</sup>M. J. Lederer, B. Luther-Davies, H. H. Tan, C. Jagadish, M. Haiml, U. Siegner, and U. Keller (unpublished).

<sup>11</sup>B. Hecht, H. Bielefeldt, Y. Inouye, and D. W. Pohl, *J. Appl. Phys.* **81**, 2492 (1997).

<sup>12</sup>M. Lamsdorf, J. Kuhl, J. Rosenzweig, A. Axmann, and J. Schneider, *Appl. Phys. Lett.* **58**, 1881 (1991).

<sup>13</sup>A. Richter, G. Brehme, M. Süptitz, C. Lienau, T. Elsässer, M. Ramsteiner, R. Nötzel, and K. H. Ploog, *Phys. Rev. Lett.* **79**, 2145 (1997).

<sup>14</sup>A. Olsson, D. J. Erskine, Z. Y. Xu, A. Schremer, and C. L. Tang, *Appl. Phys. Lett.* **41**, 659 (1982).